ISSN 1990-7931, Russian Journal of Physical Chemistry B, 2010, Vol. 4, No. 6, pp. 985–994. © Pleiades Publishing, Ltd., 2010.
Original Russian Text © V.Ya. Basevich, A.A. Belyaev, V.S. Posvyanskii, S.M. Frolov, 2010, published in Khimicheskaya Fizika, 2010, Vol. 29, No. 12, pp. 40–49.

COMBUSTION, EXPLOSION, AND SHOCK WAVES

Mechanism of the Oxidation and Combustion of Normal Paraffin Hydrocarbons: Transition from C_1–C_6 to C_7H_{16}

V. Ya. Basevich, A. A. Belyaev, V. S. Posvyanskii, and S. M. Frolov

Semenov Institute of Chemical Physics, Russian Academy of Sciences, Moscow, 119991 Russia

e-mail: basevich@center.chph.ras.ru

Received May 24, 2010

Abstract—A previously proposed algorithm for constructing an optimal mechanism of the high- and low-temperature oxidation and combustion of normal paraffin hydrocarbons was used, which includes the major processes that determine the rate of reaction and the formation of the main intermediate and final products. The mechanism has the status of a nonempirical detailed mechanism, since all the constituent elementary reactions have a kinetic substantiation. The mechanism has two specific features: it included no reactions of so-called double addition of oxygen and no isomeric compounds and derivatives thereof as intermediate species. Realization of this algorithm leads to fairly compact models, a circumstance important for studies of chemical processes involving paraffin hydrocarbons C_n with large n. Previously, based on this algorithm, compact mechanisms of oxidation and combustion of propane, *n*-butane, *n*-pentane, and *n*-hexane were constructed. In this paper, we develop a nonempirical detailed mechanism of oxidation and combustion of *n*-heptane. The most important feature of the new mechanism is its ability to predict the staging of the process in the form of cool and blue flames at low autoignition temperatures. A comparison of the simulation results with the available experimental data is conducted.

Keywords: paraffin hydrocarbons C_1–C_7, oxidation, combustion, kinetics.

DOI: 10.1134/S1990793110060175

INTRODUCTION

In recent years, detailed mechanisms of the oxidation and combustion of higher hydrocarbons have been proposed, which include hundreds of species and thousands of elementary chemical reactions. Such mechanisms allow for a variety of intermediate stable molecules and radicals in the reactions of hydrocarbons. For example, in [1], heptane oxidation was described by a scheme composed of 2300 reactions involving 650 species, whereas the oxidation of *n*-decane was simulated using 3872 reactions with 715 species. Despite the undeniable advantages of detailed mechanisms, their application to solving multidimensional problems of combustion gas dynamics is hindered by arduous computational demands.

However, if we considered all possible isomers of the species involved, and all the reactions between all the species, we could see that the size of the mechanisms described in [1, 2] could be far surpassed (e.g., due to the inclusion of polycyclic aromatic hydrocarbons, soot, fullerenes, vibrationally excited molecules, the reactions of their formation and consumption, etc.).

In addition, there is uncertainty in the construction of such mechanisms, since there are no many of the necessary and sufficiently validated data on the thermochemistry and reaction rates. It affects their kinetic validity and accuracy. Finally, in all known publications, there is no information on the applicability of the proposed detailed kinetic mechanisms to describing the multistage low-temperature oxidation of hydrocarbons [3], accompanied by the emergence of not only cool but also blue flames [4, 5].

Monograph [3] and papers [4, 5] contain experimental pressure recordings in a closed vessel during the multistage autoignition of mixtures of iso-octane and *n*-heptane with air. The pressure time history (Fig. 1) clearly shows three stages of autoignition: (1) a cool flame with time delay τ_1, (2) a blue flame, and (3) a hot explosion. The duration of the first and second stages (indicated by arrows) corresponds to a hot explosion delay τ_2 (the authors of [4] gave another explanation for these effects, but already in [3] the concept of multistage self-ignition was introduced). The total autoignition delay time can be presented as

$$\tau_i = \tau_1 + \tau_2.$$

These effects are not only actually exist but also play an important role, manifesting themselves as preflame processes in reciprocating internal combustion engines; therefore, detailed kinetic mechanisms for hydrocarbon oxidation, of course, should reproduce them and describe their sensitivity to external conditions.

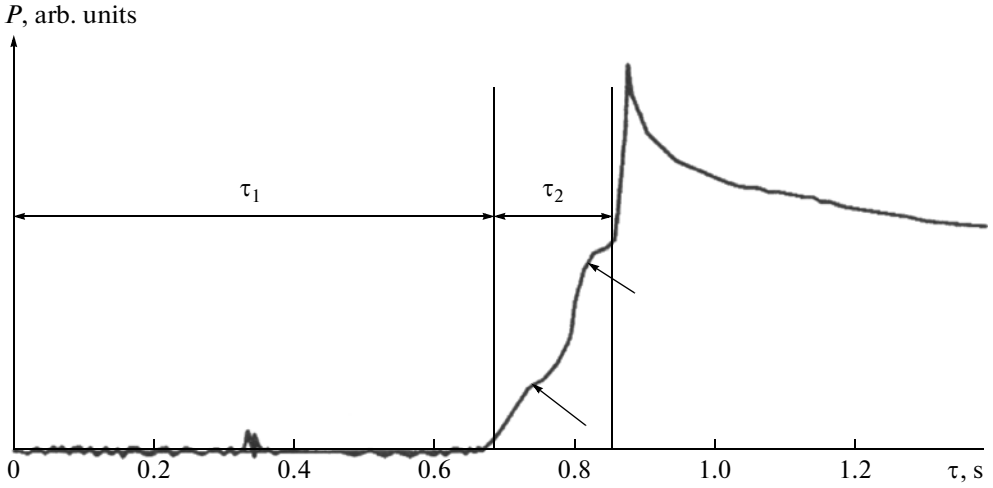

Fig. 1. Pressure record during the autoignition of an air–*n*-heptane mixture at $T_0 = 573$ K and $P_0 = 1.5$ atm [4].

Thus, the known detailed kinetic mechanisms are, as a rule, not comprehensive and, to some extent, limited. Meanwhile, for specific problems in which only the main processes that determine the reaction rate and the formation of key intermediates and final products should be taken into account, a key interest lies in developing optimal mechanisms of the oxidation and combustion of hydrocarbons rather than maximum ones. Such mechanisms, even if they are small enough, do not lose their status of nonempirical detailed mechanisms until all the components of elementary reactions have a kinetic substantiation. In other words, in simulating the oxidation and combustion of hydrocarbons, it is always possible to non-extensively construct mechanisms with purposeful limitation of the variety of products and reactions but with preservation of the main channels of the process and fundamentally important types of elementary reactions.

The reactions of paraffin hydrocarbons are known to demonstrate a certain commonality in their phenomenological description of [3–5]. This allows one to use the algorithm proposed in [6–9] (and employed previously to develop the mechanism of the oxidation and combustion of paraffin hydrocarbons (from propane to *n*-hexane)) to construct a mechanism of oxidation and combustion of the next member of the homologous series: *n*-heptane. The algorithm developed in [6–9] making use of the principle of nonextensive construction of mechanisms is based on two assumptions: low-temperature chain branching is described by reactions with addition of one oxygen; reaction pathways via the oxidation of isomeric forms can be excluded from consideration because they are slower than oxidation of non-isomeric species. Note that mechanisms of C_7H_{16} oxidation have been repeatedly proposed earlier (see, e.g., [10, 11]), but, as in the aforementioned cases, has not been demonstrated to adequately describe the multistage oxidation of hydrocarbons with the formation of not only cool but also blue flames during autoignition. Construction of an optimal mechanism of C_7H_{16} oxidation based on the non-extensive principle and exhibiting the stages of cool and blue flames during low-temperature autoignition is necessary and important for developing optimal mechanisms of the oxidation of more complex hydrocarbons (C_nH_{2n+2} with $n > 7$).

CONSTRUCTION OF THE MECHANISM

According to the algorithm described in [6–9], developing a kinetic mechanism for the C_nH_{2n+2} hydrocarbon is based on a mechanism for the preceding analogue in the homologous series, $C_{(n-1)}H_{2(n-1)+2}$. This applies to the reactants and reactions. For *n*-heptane, the preceding analogue in the homologous series is *n*-hexane; therefore, as a basis, we used the mechanism of the oxidation and combustion of C_1–C_6, which includes 72 species and 499 reactions [9]. The mechanism of the oxidation of *n*-hexane was extended to include 9 new species and 124 elementary reactions, so that the resultant mechanism consisted of 623 reactions and 81 species. The algorithm [6–9] was implemented as a computer program that selects new species, new reactions, and their Arrhenius parameters. The additional species, their enthalpies of formation ΔH°_{f298}, entropy S°_{298}, and heat capacities at constant pressure,

$$c_p = c_0 + \frac{c_1 T}{10^3} + \frac{c_2 T^2}{10^6} + \frac{c_3 T^3}{10^9},$$

as well as the additional reaction and the Arrhenius parameters are presented in Tables 1 and 2. Appearance of cool and blue flames during multistage autoignition is a typical example of critical phenomena in chemical kinetics. It is known that critical phenomena are multifunctional and manifest themselves at a cer-

Table 1. Reactants included into the mechanism of the oxidation and combustion of *n*-heptane

No.	Reactant	ΔH°_{f298}, cal/mol	S°_{298}, cal/(mol K)	c_0, cal/(mol K)	c_1, cal/(mol K^2)	c_2, cal/(mol K^3)	c_3, cal/(mol K^4)
73	C_7H_{16}	−0.445E+05	0.103E+03	0.431E+00	0.159E+03	−0.862E+02	0.182E+02
74	C_7H_{15}	0.367E+04	0.106E+03	0.207E+01	0.150E+03	−0.840E+02	0.207E+02
75	$C_7H_{15}O_2$	−0.240E+05	0.125E+03	0.290E+01	0.175E+03	−0.106E+03	0.294E+02
76	$C_7H_{15}O_2H$	−0.597E+05	0.123E+03	0.258E+01	0.178E+03	−0.106E+03	0.288E+02
77	$C_7H_{15}O$	−0.262E+05	0.116E+03	0.178E+00	0.175E+03	−0.107E+03	0.315E+02
78	$C_6H_{13}CHO$	−0.649E+05	0.111E+03	0.112E+02	0.110E+03	−0.678E+01	−0.351E+02
79	$C_7H_{13}CO$	−0.297E+05	0.112E+03	0.112E+02	0.110E+03	−0.678E+01	−0.351E+02
80	C_7H_{14}	−0.148E+05	0.102E+03	0.237E+01	0.142E+03	−0.760E+02	0.158E+02
81	C_7H_{13}	0.293E+05	0.101E+03	0.298E+01	0.128E+03	−0.648E+02	0.127E+02

tain ratio between the rates of different elementary reactions. Therefore, the kinetic modeling of these phenomena requires additional analysis and selection of the rate constants of key reactions over the range of theoretically allowable values that do not exceed the experimental error. In other words, approximate values of the key rate constants not always ensure an adequate description of the observed critical phenomena. In the resulting mechanism of oxidation of *n*-heptane, the adjustment of the rate constants was needed only for a limited number of processes: the reactions of *n*-heptane with hydroperoxide radicals and heptyl radical reaction with molecular oxygen.

VALIDATION OF THE MECHANISM

Experiments on the Spontaneous Ignition of Gas Mixtures

The predictive ability of the mechanism was tested by comparing the calculation results with experimental data on various processes of oxidation and autoignition of C_7H_{16}. The calculations were performed by the standard kinetic program from [6–9].

The calculated time dependence of the temperature for the autoignition of an *n*-heptane–air mixture for the conditions specified in Fig. 1 is displayed in Fig. 2. The development of the process shown in Fig. 2 is typical of low and moderately high initial temperatures. The first stepwise rise in temperature is associated with the emergence of a cool flame. After some time, the cool flame gives way to a blue flame, followed by a hot explosion, with the temperature rising to above 2300 K; i.e., manifestations of multistage ignition are observed. The acceleration of the cool flame reaction is a consequence of chain branching in the course of the decomposition of an alkyl hydroperoxide (here, heptyl hydroperoxide $C_7H_{15}O_2H$) to form a hydroxyl radical and an alkyloxy radical. The blue flame appears due to the chain branching associated with the decomposition of hydrogen peroxide, H_2O_2. The hot explosion is a consequence of branched-chain reaction of atomic hydrogen with molecular oxygen.

The multistage character of the process gives rise to the phenomenon of negative temperature coefficient of reaction (NTC): when, the total ignition delay time at a higher initial temperature turns out to be longer than that at a lower temperature. This can be seen from Fig. 3, which shows the temperature dependence of the ignition delay time for a stoichiometric mixture of 1.86 vol % C_7H_{16} with air at initial pressures of P_0 = 2.8–40 atm. The symbols in Fig. 3 represent the experimental data from [12–18], whereas the curves show the calculation results.

It is seen that the experimental and calculated data are in qualitative agreement. As in high-temperature experiments (to the left of the NTC region), the self-ignition apparently proceeds as a single-stage process with an exponential rise in temperature over time. Figure 4 shows a comparison of the measured [4] and cal-

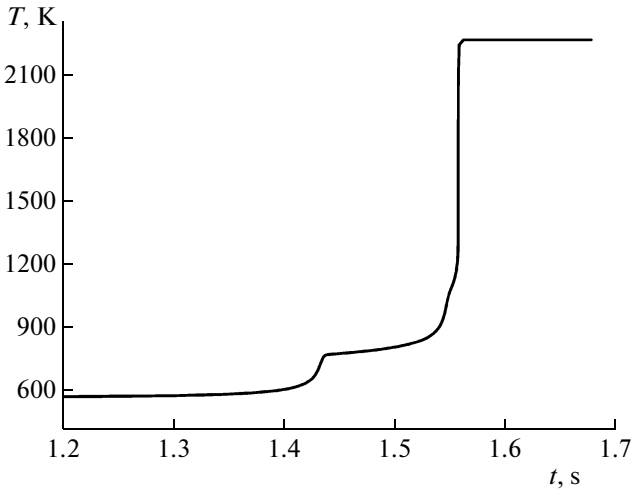

Fig. 2. Calculated time dependence of the temperature for the autoignition of a 1.86 vol % *n*-C_7H_{16}–air stoichiometric mixture at T_0 = 573 K and P_0 = 1.5 atm.

Table 2. Mechanism of the oxidation and combustion of *n*-heptane

No.	Reaction	*A*, l, mol, s	*E*/*R*, K
1	$C_7H_{16} + O_2 = C_7H_{15} + HO_2$	0.400E+10	0.239E+05
2	$C_7H_{16} + OH = C_7H_{15} + H_2O$	0.630E+10	0.600E+03
3	$C_7H_{16} + H = C_7H_{15} + H_2$	0.930E+11	0.403E+04
4	$C_7H_{16} + O = C_7H_{15} + OH$	0.505E+04	0.277E+04
5	$C_7H_{16} + HO_2 = C_7H_{15} + H_2O_2$	0.600E+09	0.856E+04
6	$C_7H_{14} + H = C_7H_{15}$	0.189E+10	0.315E+03
7	$C_7H_{15} + O_2 = C_7H_{14} + HO_2$	0.220E+11	0.800E+04
8	$C_7H_{15} + OH = C_7H_{14} + H_2O$	0.600E+10	0.000E+00
9	$C_7H_{16} = H + C_7H_{15}$	0.359E+14	0.376E+05
10	$C_7H_{16} = CH_3 + C_6H_{13}$	0.404E+16	0.421E+05
11	$C_7H_{16} = C_2H_5 + C_5H_{11}$	0.195E+17	0.428E+05
12	$C_7H_{16} = C_3H_{7\,+}\,C_4H_9$	0.157E+17	0.428E+05
13	$C_7H_{15} + H = C_7H_{14} + H_2$	0.600E+10	0.000E+00
14	$C_7H_{15} + CH_3 = C_7H_{14} + CH_4$	0.351E+09	–0.106E+03
15	$C_7H_{15} + C_2H_5 = C_7H_{14} + C_2H_6$	0.158E+11	0.466E+03
16	$C_7H_{15} + C_3H_7 = C_7H_{14} + C_3H_8$	0.138E+09	0.488E+03
17	$C_7H_{15} + C_4H_9 = C_7H_{14} + C_4H_{10}$	0.138E+09	0.488E+03
18	$C_7H_{15} + C_5H_{11} = C_7H_{14} + C_5H_{12}$	0.138E+09	0.488E+03
19	$C_7H_{15} + C_6H_{13} = C_7H_{14} + C_6H_{14}$	0.138E+09	0.488E+03
20	$C_7H_{15} + O = C_7H_{14} + OH$	0.200E+12	0.000E+00
21	$C_7H_{15} + O_2 = C_7H_{15}O_2$	0.400E+08	–0.500E+03
22	$C_7H_{16} + CH_3O_2 = C_7H_{15} + CH_3O_2H$	0.140E+11	0.650E+04
23	$C_7H_{16} + C_2H_5O_2 = C_7H_{15} + C_2H_5O_2H$	0.140E+11	0.650E+04
24	$C_7H_{16} + C_3H_7O_2 = C_7H_{15} + C_3H_7O_2H$	0.140E+11	0.650E+04
25	$C_7H_{16} + C_4H_9O_2 = C_7H_{15} + C_4H_{10}O_2$	0.140E+11	0.650E+04
26	$C_7H_{16} + C_5H_{11}O_2 = C_7H_{15} + C_5H_{12}O_2$	0.140E+11	0.650E+04
27	$C_7H_{16} + C_6H_{13}O_2 = C_7H_{15} + C_6H_{14}O_2$	0.140E+11	0.650E+04
28	$C_7H_{16} + C_7H_{15}O_2 = C_7H_{15} + C_7H_{16}O_2$	0.140E+11	0.650E+04
29	$C_7H_{16}O_2 = C_7H_{15}O + OH$	0.500E+16	0.200E+05
30	$C_7H_{15}O = H_2CO + C_6H_{13}$	0.158E+15	0.797E+04
31	$C_7H_{15}O = CH_3CHO + C_5H_{11}$	0.312E+15	0.113E+05
32	$C_7H_{15}O = C_2H_5CHO + C_4H_9$	0.302E+15	0.103E+05
33	$C_7H_{15}O = C_4H_8O + C_3H_7$	0.302E+15	0.103E+05
34	$C_7H_{15}O = C_5H_{10}O + C_2H_5$	0.374E+15	0.103E+05
35	$C_7H_{15}O = C_6H_{12}O + CH_3$	0.775E+14	0.108E+05
36	$C_7H_{15}O = C_7H_{14}O + H$	0.688E+12	0.626E+04
37	$C_7H_{15}O_2 + H = C_7H_{15}O + OH$	0.236E+11	–0.161E+04
38	$C_7H_{15}O_2 + CH_3 = C_7H_{15}O + CH_3O$	0.364E+09	–0.166E+03
39	$C_7H_{15}O_2 + C_2H_5 = C_7H_{15}O + C_2H_5O$	0.827E+09	–0.649E+03
40	$C_7H_{15}O_2 + C_3H_7 = C_7H_{15}O + C_3H_7O$	0.630E+09	0.000E+00
41	$C_7H_{15}O_2 + C_4H_9 = C_7H_{15}O + C_4H_9O$	0.630E+09	0.000E+00
42	$C_7H_{15}O_2 + C_5H_{11} = C_7H_{15}O + C_5H_{11}O$	0.630E+09	0.000E+00
43	$C_7H_{15}O_2 + C_6H_{13} = C_7H_{15}O + C_6H_{13}O$	0.630E+09	0.000E+00
44	$C_7H_{15}O_2 + C_7H_{15} = C_7H_{15}O + C_7H_{15}O$	0.630E+09	0.000E+00
45	$C_7H_{15}O_2 + H_2CO = C_7H_{16}O_2 + HCO$	0.320E+09	0.564E+04

Table 2. (Contd.)

No.	Reaction	*A*, l, mol, s	*E*/*R*, K
46	$C_7H_{15}O_2 + CH_3CHO = C_7H_{16}O_2 + CH_3CO$	0.315E+09	0.560E+04
47	$C_7H_{15}O_2 + C_2H_5CHO = C_7H_{16}O_2 + C_2H_5CO$	0.315E+09	0.554E+04
48	$C_7H_{15}O_2 + C_4H_8O = C_7H_{16}O_2 + C_4H_7O$	0.315E+09	0.554E+04
49	$C_7H_{15}O_2 + C_5H_{10}O = C_7H_{16}O_2 + C_5H_9O$	0.315E+09	0.554E+04
50	$C_7H_{15}O_2 + C_6H_{12}O = C_7H_{16}O_2 + C_6H_{11}O$	0.315E+09	0.554E+04
51	$C_7H_{15}O_2 + C_7H_{14}O = C_7H_{16}O_2 + C_7H_{13}O$	0.315E+09	0.554E+04
52	$C_7H_{15} + HO_2 = C_7H_{15}O + OH$	0.300E+11	0.000E+00
53	$C_7H_{15} + O_2 = C_7H_{14}O + OH$	0.400E+10	0.900E+04
54	$C_7H_{15} + C_2H_5 = C_7H_{16} + C_2H_4$	0.625E+09	0.335E+03
55	$C_7H_{15} + C_3H_7 = C_7H_{16} + C_3H_6$	0.190E+10	0.000E+00
56	$C_7H_{15} + C_4H_9 = C_7H_{16} + C_4H_8$	0.190E+10	0.000E+00
57	$C_7H_{15} + C_5H_{11} = C_7H_{16} + C_5H_{10}$	0.190E+10	0.000E+00
58	$C_7H_{15} + C_6H_{13} = C_7H_{16} + C_6H_{12}$	0.190E+10	0.000E+00
59	$C_7H_{15} + C_7H_{15} = C_7H_{16} + C_7H_{14}$	0.190E+10	0.000E+00
60	$C_7H_{15} + O_2 = H_2CO + C_6H_{13}O$	0.400E+11	0.700E+04
61	$C_7H_{15} + O_2 = CH_3CHO + C_5H_{11}O$	0.400E+11	0.700E+04
62	$C_7H_{15} + O_2 = C_2H_5CHO + C_4H_9O$	0.400E+11	0.700E+04
63	$C_7H_{15} + O_2 = C_4H_8O + C_3H_7O$	0.400E+11	0.700E+04
64	$C_7H_{15} + O_2 = C_5H_{10}O + C_2H_5O$	0.400E+11	0.700E+04
65	$C_7H_{15} + O_2 = C_6H_{12}O + CH_3O$	0.400E+11	0.700E+04
66	$C_7H_{15} + OH = CH_3 + C_6H_{13}O$	0.184E+11	−0.194E+04
67	$C_7H_{15} + OH = C_2H_5 + C_5H_{11}O$	0.891E+11	0.417E+03
68	$C_7H_{15} + OH = C_3H_7 + C_4H_9O$	0.719E+11	0.413E+03
69	$C_7H_{15} + OH = C_4H_9 + C_3H_7O$	0.719E+11	0.413E+03
70	$C_7H_{15} + OH = C_5H_{11} + C_2H_5O$	0.117E+12	−0.232E+03
71	$C_7H_{15} + OH = C_6H_{13} + CH_3O$	0.107E+11	0.480E+03
72	$C_7H_{15} + H = CH_3 + C_6H_{13}$	0.388E+11	0.546E+03
73	$C_7H_{15} + H = C_2H_5 + C_5H_{11}$	0.187E+12	0.318E+03
74	$C_7H_{15} + H = C_3H_7 + C_4H_9$	0.151E+12	0.314E+03
75	$C_7H_{15} + H = CH_2 + C_6H_{14}$	0.423E+08	0.302E+04
76	$C_7H_{15} + H = C_2H_4 + C_5H_{12}$	0.722E+07	−0.641E+04
77	$C_7H_{15} + H = C_3H_6 + C_4H_{10}$	0.177E+08	−0.675E+04
78	$C_7H_{15} + H = C_4H_8 + C_3H_8$	0.177E+08	−0.675E+04
79	$C_7H_{15} + H = C_5H_{10} + C_2H_6$	0.251E+10	−0.677E+04
80	$C_7H_{15} + H = C_6H_{12} + CH_4$	0.116E+08	−0.711E+04
81	$C_7H_{15} + O = H + C_7H_{14}O$	0.702E+09	0.565E+03
82	$C_7H_{15} + O = CH_3 + C_6H_{12}O$	0.790E+11	−0.952E+03
83	$C_7H_{15} + O = C_2H_5 + C_5H_{10}O$	0.381E+12	−0.118E+04
84	$C_7H_{15} + O = C_3H_7 + C_4H_8O$	0.308E+12	−0.118E+04
85	$C_7H_{15} + O = C_4H_9 + C_2H_5CHO$	0.308E+12	−0.118E+04
86	$C_7H_{15} + O = C_5H_{11} + CH_3CHO$	0.318E+12	−0.111E+04
87	$C_7H_{15} + O = C_6H_{13} + H_2CO$	0.162E+12	−0.352E+01
88	$C_7H_{13}O + HO_2 = C_7H_{14}O + O_2$	0.530E+08	0.000E+00
89	$C_7H_{14}O + OH = C_7H_{13}O + H_2O$	0.100E+11	0.000E+00
90	$C_7H_{14}O + H = C_7H_{13}O + H_2$	0.140E+11	0.165E+04

Table 2. (Contd.)

No.	Reaction	A, l, mol, s	E/R, K
91	$C_7H_{14}O + O = C_7H_{13}O + OH$	0.568E+10	0.780E+03
92	$C_7H_{14}O + HO_2 = C_7H_{13}O + H_2O_2$	0.600E+09	0.500E+04
93	$C_6H_{13} + HCO = C_7H_{14}O$	0.223E+11	0.352E+01
94	$C_6H_{13} + CO = C_7H_{13}O$	0.187E+09	0.242E+04
95	$C_7H_{13}O + H = C_6H_{13} + HCO$	0.485E+10	0.240E+04
96	$C_7H_{13}O + O = C_6H_{13}O + CO$	0.369E+10	0.646E+03
97	$C_7H_{14} + OH = C_7H_{13} + H_2O$	0.900E+11	0.325E+04
98	$C_7H_{13} + H_2 = C_7H_{14} + H$	0.853E+11	0.533E+04
99	$C_7H_{13} + O_2 = C_5H_{11}O_2 + C_2H_2$	0.242E+11	0.396E+04
100	$C_7H_{14} + HCO = C_7H_{13} + H_2CO$	0.600E+11	0.900E+04
101	$C_7H_{14} + CH_3 = C_7H_{13} + CH_4$	0.107E+09	0.268E+04
102	$C_7H_{14} + C_2H_5 = C_7H_{13} + C_2H_6$	0.481E+10	0.325E+04
103	$C_7H_{14} + C_3H_7 = C_7H_{13} + C_3H_8$	0.420E+08	0.328E+04
104	$C_7H_{14} + C_4H_9 = C_7H_{13} + C_4H_{10}$	0.420E+08	0.328E+04
105	$C_7H_{14} + C_5H_{11} = C_7H_{13} + C_5H_{12}$	0.420E+08	0.328E+04
106	$C_7H_{14} + C_6H_{13} = C_7H_{13} + C_6H_{14}$	0.420E+08	0.328E+04
107	$C_5H_{11} + C_2H_2 = C_7H_{13}$	0.141E+10	0.143E+04
108	$C_7H_{14} = C_2H_3 + C_5H_{11}$	0.390E+14	0.379E+05
109	$C_7H_{14} = C_3H_5 + C_4H_9$	0.113E+14	0.446E+05
110	$C_7H_{14} = C_4H_7 + C_3H_7$	0.113E+14	0.446E+05
111	$C_7H_{14} = C_5H_9 + C_2H_5$	0.140E+14	0.446E+05
112	$C_7H_{14} = C_6H_{11} + CH_3$	0.289E+13	0.439E+05
113	$C_7H_{14} + O_2 = C_7H_{13} + HO_2$	0.600E+11	0.236E+05
114	$C_7H_{14} + O = C_6H_{13} + HCO$	0.404E+10	0.226E+03
115	$C_7H_{13} + OH = C_6H_{13} + HCO$	0.485E+10	−0.352E+01
116	$C_7H_{13} + H = C_5H_{12} + C_2H_2$	0.917E+10	0.362E+03
117	$C_7H_{13} + O = C_6H_{13} + CO$	0.485E+10	−0.352E+01
118	$C_7H_{13} + O = C_5H_{11}O + C_2H_2$	0.405E+11	−0.662E+02
119	$CH_3 + C_6H_{13} = C_7H_{14} + H_2$	0.248E+14	0.191E+05
120	$C_2H_5 + C_5H_{11} = C_7H_{14} + H_2$	0.513E+13	0.193E+05
121	$C_3H_7 + C_4H_9 = C_7H_{14} + H_2$	0.636E+13	0.193E+05
122	$C_7H_{14} + H + H = CH_3 + C_6H_{13}$	0.145E+07	−0.500E+04
123	$C_7H_{14} + H + H = C_2H_5 + C_5H_{11}$	0.701E+07	−0.523E+04
124	$C_7H_{14} + H + H = C_3H_7 + C_4H_9$	0.566E+07	−0.524E+04
(followed by the mechanism of the oxidation and combustion of C_1–C_6)			

culated autoignition delay times for a rich mixture of 2.32 vol% C_7H_{16} with air at $T_0 = 533$ K and relatively low pressures. As is seen, at a pressure of 0.4 atm, both experiment and calculations show that the oxidation reaction is limited to only the appearance of a cool flame. The pressure of 1.7 atm separates the regions of cool-flame oxidation and hot explosion. Here, we can see qualitative agreement between the experimental and calculated data on the time delay of cool flame appearance τ_1 and the total delay τ_i.

According to Fig. 5, the self-ignition of a 2.32 vol % C_7H_{16}–air mixture in the hot-explosion region might be perceived as a single-stage process with a delay time of $\tau_i \sim 4$ s. However, calculations showed that hundredths of a second before the ignition, a cool and a blue flame arise, at 3.678 and 3.687 s, respectively. This is clearly seen from the behavior of the concentrations of peroxides and hydroxyl radicals (Figs. 6 and 7, respectively). Because integral characteristics of the process are normally measured, such a separation of

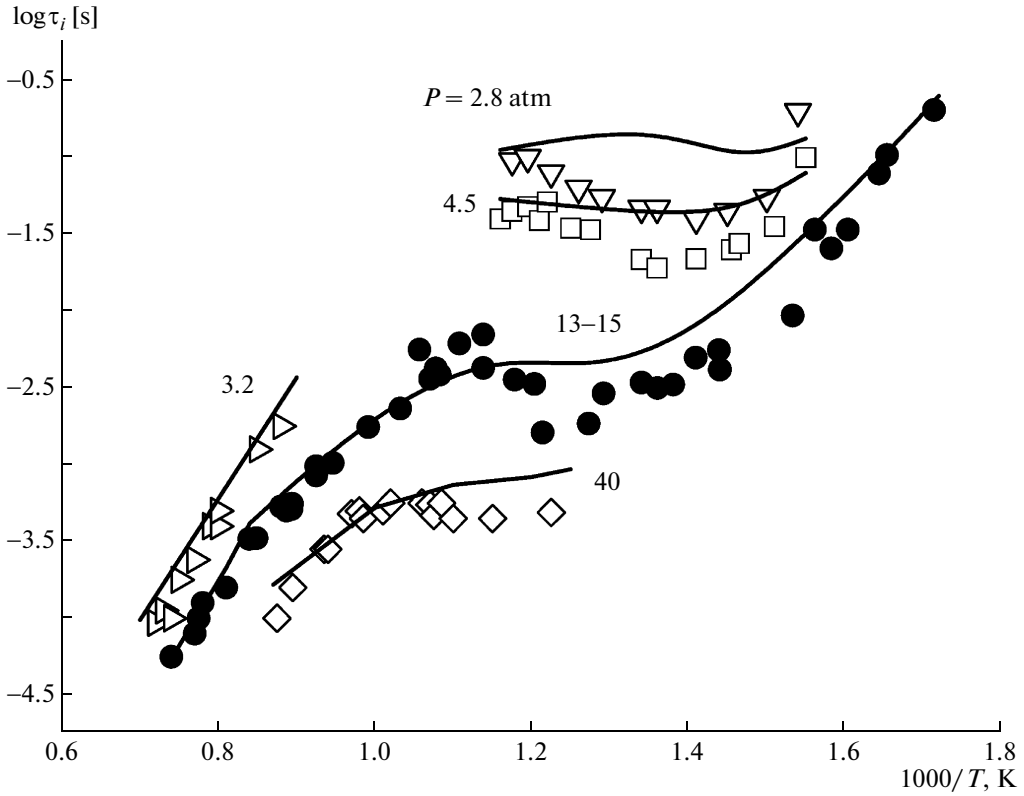

Fig. 3. Measured (symbols, [12–18]) and calculated (lines) temperature dependences of the ignition delay time for a 1.86 vol % n-C_7H_{16}–air stoichiometric mixture at $P_0 = 2.8$–40 atm.

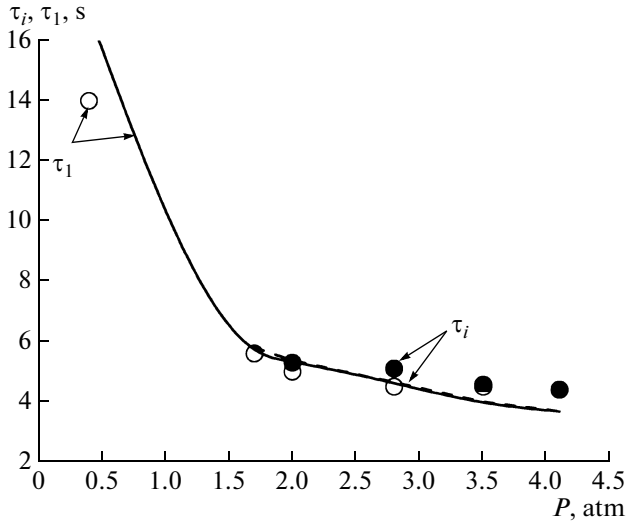

Fig. 4. Measured (symbols, [4]) and calculated (lines) pressure dependences of the ignition delay time for a 2.32 vol % n-C_7H_{16}–air mixture at an initial temperature of $T_0 = 533$ K: τ_1 the delay time of the cool flame and τ_i is the overall delay time.

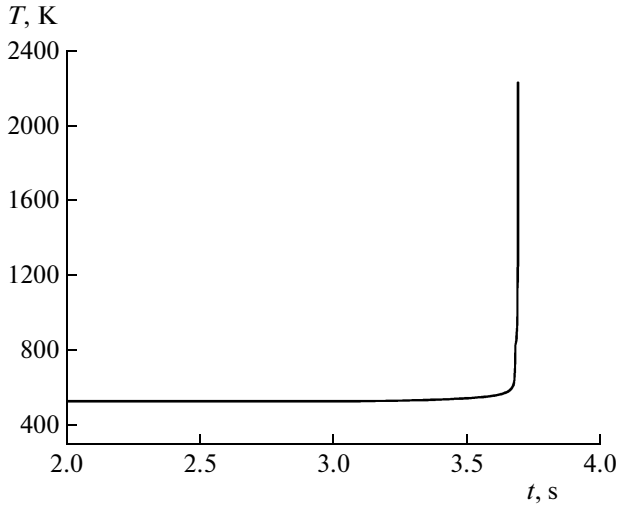

Fig. 5. Calculated time dependence of the temperature for the autoignition of a 2.32 vol % n-C_7H_{16}–air mixture at $T_0 = 533$ K and $P_0 = 4.1$ atm.

the individual stages cannot be detected for various reasons (for example, due to temperature nonuniformities). In reality, however, the staging is always realized.

Simulations of the oxidation of n-heptane in the conditions of the experiments performed in [4] make it possible to quantitatively reproduce experimental pressure recordings during multistage autoignition

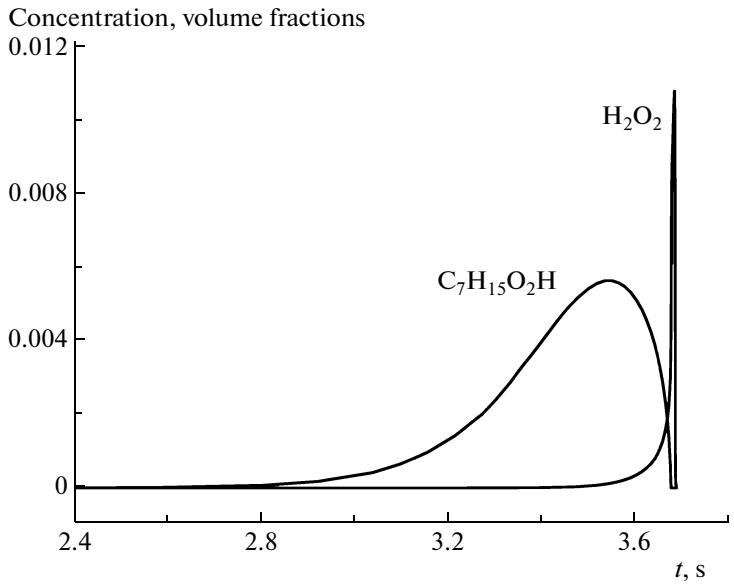

Fig. 6. Calculated time dependences of the concentrations of peroxides for the autoignition of a 2.32 vol % n-C_7H_{16}–air mixture at $T_0 = 533$ K and $P_0 = 4.1$ atm.

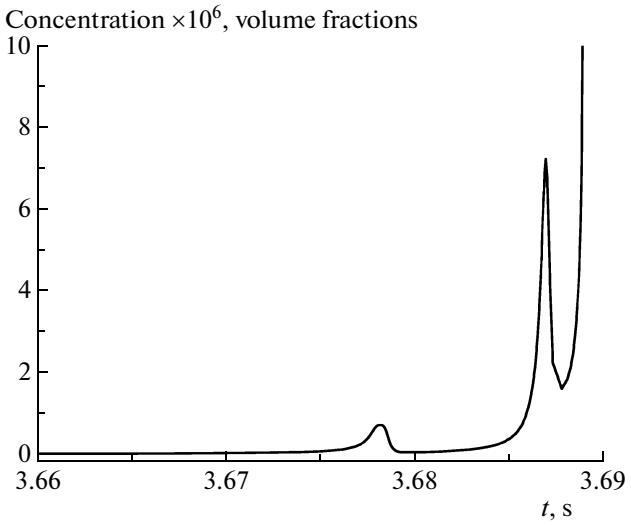

Fig. 7. Calculated time dependences of the concentrations of OH radicals for the autoignition of a 2.32 vol % n-C_7H_{16}–air mixture at $T_0 = 533$ K and $P_0 = 4.1$ atm.

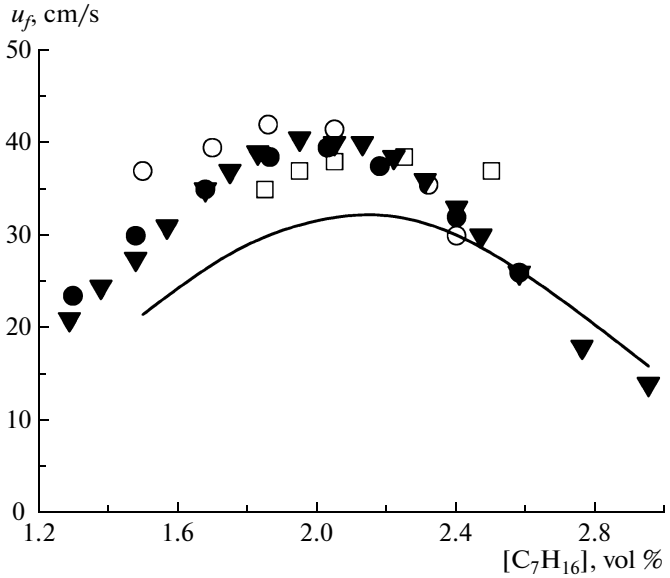

Fig. 8. Calculated (line) and measured (symbols) dependences of the laminar flame speed u_n on the concentration of n-C_7H_{16} in a mixture with air at normal initial conditions: ○ [22], □ [23], ● [24], and ▼ [25].

with the appearance of cool and blue flames (simulations of this kind were carried out in [19] using an extended semiempirical mechanism). Experimental data on blue flames in the oxidation of *n*-heptane are given in [3]. More recently, blue flames were registered in a variety of fuel mixtures containing *n*-heptane [20], but the authors [20] gave the blue flame a new name, preignition, and proposed a complex kinetic mechanism of its realization, involving, in particular, reactions with aromatic structures, a mechanism that fundamentally differs from that proposed in the present work.

Experiments on Laminar Flame Propagation

For further verification of the kinetic mechanism, we performed calculations to determine the laminar flame speed u_f in an *n*-heptane–air mixture under normal conditions (atmospheric pressure, initial temperature $T_0 = 293$ K). Calculations were performed as

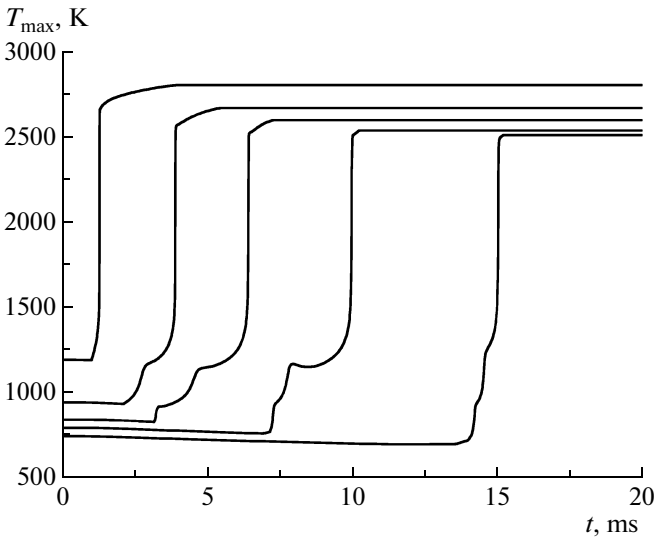

Fig. 9. Calculated time dependences of the maximum temperature for the autoignition of a stoichiometric ($\Phi = 1$) air–n-C_7H_{16} droplet suspension at $P_0 = 20$ atm, initial droplet diameter of $d_0 = 60$ μm, and various initial temperatures of the ambient air.

described in [21]. A comparison of the calculation results with the experimental data from [22–25] is shown in Fig. 8.

Experiments on the Spontaneous Ignition of Droplets

The developed detailed kinetic mechanism was also applied to calculating the ignition and combustion of n-heptane droplets under microgravity conditions. The calculations were performed using one-dimensional unsteady equations of conservation of mass, chemical components, and energy for the gas and condensed phases with matching of the solutions on the spherical surface of the droplet. A detailed description of the mathematical model and calculation method are given in [26, 27]. The temperature of the air around the droplet was set constant, T_0, whereas the initial temperature of the liquid was assumed to be 293 K. The radius of the computational domain R was considered sufficiently large compared with the initial droplet radius r_0. According to [26, 27], any selected value of R corresponds to a certain fuel-to oxidizer equivalence ratio Φ in a homogeneous monodisperse gas–droplet suspension.

Table 3. Autoignition delay time for single n-heptane droplets at a pressure of 1 atm

Initial droplet diameter, μm	Air temperature, K	Autoignition delay time, s	
		experiment	calculation
700	1000	0.30 [28]	0.18
1000	960	0.58 [29]	0.27

After the induction period, the gas-fuel vapor self-ignited at a certain distance from the center of the droplet. Solving the problem for single droplets of various sizes and gas–droplet suspensions (uniform and monodisperse) over a wide range of pressures, and initial air temperatures, and initial mixture compositions Φ showed that, under certain conditions, the autoignition of droplets exhibit the same multi-staging as the autoignition of respective gas mixtures does (Fig. 9).

A comparison of the calculated induction periods of self-ignition with the measured value for single droplets under microgravity conditions is presented in Table 3.

CONCLUSIONS

Thus, a new nonempirical detailed mechanism of the oxidation and combustion of n-heptane was developed. The most important feature of this mechanism is its ability to predict the appearance of cool and blue flames during low-temperature autoignition. Calculations of the ignition and combustion of gas mixtures and droplets of n-heptane over a wide range of initial conditions were performed, and the results were compared to the respective experimental data. In general, a satisfactory qualitative and quantitative agreement between the results of calculations and experiments was achieved. This means that the principle of non-extensive construction of kinetic mechanisms with the target constraint variety of products and reactions, but the preservation of the main channels of the process and fundamentally important types of elementary acts, seem to apply to the description of oxidation and combustion of n-heptane.

ACKNOWLEDGMENTS

This work was supported by the State Contract no. P502 and the Russian Foundation for Basic Research, project no. 08-08-00068.

REFERENCES

1. C. Chevalier, P. Louessard, U. C. Muller, and J. Warnatz, in *Proc. Joint Meeting of Sov. Ital. Sections Comb. Inst.* (Combustion Inst., Pisa, 1990), p. 5.
2. F. Buda, R. Bounaceur, et al., Combust. Flame **142**, 170 (2005).
3. A. S. Sokolik, *Self-Ignition, Flame, and Detonation in Gases* (Akad. Nauk SSSR, Moscow, 1960) [in Russian].
4. A. S. Sokolik and S. A. Yantovskii, Zh. Fiz. Khim. **20**, 13 (1946).
5. V. Ya. Basevich and S. M. Frolov, Usp. Khim. **76**, 927 (2007).
6. V. Ya. Basevich, V. I. Vedeneev, S. M. Frolov, and L. B. Romanovich, Khim. Fiz. **25** (11), 87 (2006).
7. V. Ya. Basevich, A. A. Belyaev, and S. M. Frolov, Khim. Fiz. **26** (7), 37 (2007) [Russ. J. Phys. Chem. B **1**, 493 (2007)].

8. V. Ya. Basevich, A. A. Belyaev, and S. M. Frolov, Khim. Fiz. **28** (8), 59 (2009) [Russ. J. Phys. Chem. B **3**, 629 (2009)].
9. V. Ya. Basevich, A. A. Belyaev, and S. M. Frolov, Khim. Fiz. **29** (7), 71 (2010) [Russ. J. Phys. Chem. B **4**, 694 (2010)].
10. H. J. Curran, P. Gaffuri, W. J. Pitz, and C. K. Westbrook, Combust. Flame **114**, 149 (1998).
11. M. Chaos, A. Kazakov, Z. Zhao, and F. I. Dryer, Int. J. Chem. Kinet. **39**, 399 (2007).
12. H. Rogener, Z. Elektrochem. Angew. Phys. Chem. **53**, 389 (1949).
13. C. F. Taylor, E. S. Taylor, J. S. Livengood, et al., SAE Quart. Trans. **4**, 232 (1950).
14. H. Ciezki and G. Adomeit, in *Proc. 16th Intern. Symp. on Shock Tubes and Waves* (Niagara Falls, 1987), p. 481.
15. Ch. Poppe, M. Schreber, and J. F. Griffith, in *Proc. Joint Meeting British and German Sections of The Combustion Institute* (Cambridge, 1993), p. 1993.
16. H. Ciezki and G. Adomeit, Combust. Flame **93**, 421 (1993).
17. R. Minetti, M. Carlier, M. Ribaucour, et al., Combust. Flame **102**, 298 (1995).
18. B. M. Gauthier, D. F. Davidson, and R. K. Hanson, Combust. Flame **139**, 300 (2004).
19. V. Ya. Basevich, V. I. Vedeneev, S. M. Frolov, and L. B. Romanovich, Khim. Fiz. **23** (1), 50 (2004).
20. H. Machrafi and S. Cavadias, Combust. Flame **155**, 557 (2008).
21. A. A. Belyaev and V. S. Posvyanskii, in *Algorithms and Programs*, Inform. Byull. Gos. Fonda Algoritmov Programm SSSR (1985), No. 3, p. 35.
22. M. Gerstein, O. Levin, and E. L. Wang, JACS **73**, 418 (1951).
23. G. J. Gibbs and H. F. Calcote, J. Chem. Eng. Data **4**, 226 (1959).
24. S. G. Davis and C. K. Law, Proc. Combust. Inst. **27**, 521 (1998).
25. Y. Hyang, C. J. Sung, and J. A. Eng, Combust. Flame **139**, 239 (2004).
26. S. M. Frolov, V. S. Posvyanskii, V. Ya. Basevich, et al., Khim. Fiz. **23** (4), 75 (2004).
27. S. M. Frolov, V. Ya. Basevich, A. A. Belyaev, V. S. Posvyanskii, and V. A. Smetanyuk, in *Combustion and Pollution: Environmental Impact*, Ed. by G. D. Roy, S. M. Frolov, and A. M. Starik (Torus, Moscow, 2005), p. 117 [in Russian].
28. M. Takei, H. Kobayashi, and T. Niioka, Int. J. Micrograv. Res. Appl. Micrograv. Sci. Technol. **6** (3), 184 (1993).
29. T. Niioka, H. Kobayashi, and D. Mito, in *Proc. IVTAM Symp. on Mechanics and Combustion of Droplet and Sprays* (Tainan, 1994), p. 367.